JOURNAL OF SOLID STATE CHEMISTRY 109, 391–400 (1994)

Synthesis and Structure of a Compositely Modulated Solid Solution in the Zirconium Nitride Oxide Fluoride System

Siegbert Schmid[1] and Ray L. Withers

Research School of Chemistry, Australian National University, Canberra, ACT, 0200, Australia

Received June 3, 1993; accepted September 14, 1993

The phase $Zr(N,O,F)_x$ has been studied by X-ray powder diffraction and transmission electron microscopy. It had previously been described as an oxygen free nitride fluoride and the structure of one composition from the solid solution field solved as a so-called Vernier superstructure approximation. More correctly the phase should be described as an incommensurate, compositely modulated structure, with a continuously variable, composition-dependent, primary modulation wave-vector. The total anion to cation ratio can be uniquely determined from careful measurement of diffraction patterns and is shown to be continuously variable and to range between 2.12 and 2.25. The cell parameters of the component substructures are determined and show a linear dependence upon the anion to cation ratio. Apparent valence calculations are used to investigate anion ordering.

1. INTRODUCTION

Although the first nitride fluoride was synthesized in 1966 by Juza *et al.* (1) a much wider interest in nitride fluorides was created in 1967 when Andersson (2) expressed the idea that nitride fluorides can be regarded as pseudooxides (because of the isoelectronic relation between $2O^{2-}$ and $F^- + N^{3-}$ and their similar ionic radii) and might even be isostructural with the corresponding oxides. Subsequently more nitride fluorides have been synthesized (3–5) and most are in fact structurally related to the oxides. In 1973, Jung and Juza (3) first reported the synthesis of a zirconium nitride fluoride ZrN_xF_{4-3x} solid solution. It was reported to have a fairly wide composition range from $x = 0.906$ to $x = 0.936$. They were not only able to synthesize powder specimens but also managed to grow single crystals of various compositions. Precession photographs of these various crystals always showed a multitude of satellite reflections in addition to a set of strong subcell reflections. Jung and Juza interpreted the strong subcell reflections as arising from an underlying fluorite-type parent structure and the satellite reflections as some sort of superstructure thereof. While they were aware that the spacing between neighboring satellite reflections was often not constant, they were not aware that all such patterns can be coherently indexed as an incommensurate, compositely modulated structure, with a continuously variable, composition-dependent, primary modulation wave-vector.

Subsequently an attempt was made to solve a 27-times superstructure (3). With this result and those of Bevan and Mann (6) on the apparently isostructural yttrium oxide fluoride system YO_xF_{3-2x}, $0.78 \leq x \leq 0.87$, Hyde *et al.* (7) were able to provide a rational descriptive framework for such systems via the introduction of the concept of Vernier phases, anion excess, fluorite-related structures (8, 9). Instead of describing the fluorite structure as a primitive cubic anion array with cations occupying half of the cubic sites it was described as a cubic close packed cation array with anions in all the tetrahedral sites, i.e., anion centered XM_4 tetrahedra sharing all edges. The structure was then split into tetragonal layers of tetrahedra (one tetrahedron thick; stoichiometry XM) and notional 4^4 layers of anions in between (stoichiometry X) (see Fig. 7, Chapt. 12 of (8)). Deforming the 4^4 layers of anions to 3^6 nets resulted in the possibility of accommodating more anions (ideally $2/\sqrt{3}$ more giving stoichiometry $X_{1.1547}$) and gave rise to an overall composition of $MX_{2.1547}$. The generally observed composition range of such Vernier phases, $MX_{2+\delta}$ with $0.13 \leq \delta \leq 0.22$, was then accommodated by altering the average periodicity along **c** of the substructure based upon the 3^6 layers (the so-called H substructure) relative to the average periodicity along **c** of the substructure based upon the one tetrahedron thick, pseudotetragonal layers (the so-called Q substructure): $q\mathbf{c}_H = p\mathbf{c}_Q$, i.e., q repeats of the former being presumed to correspond to p repeats of the latter (p,q both integers—hence the name Vernier phases; see Fig. 1). Note that the setting we are using corresponds to that drawn in Fig. 8 of Chapt. 12 of (8). The cation array thereby remains almost unaffected (fcc) and most anions still retain a coordination number of 4.

[1] To whom correspondence should be addressed.

0022-4596/94 $6.00

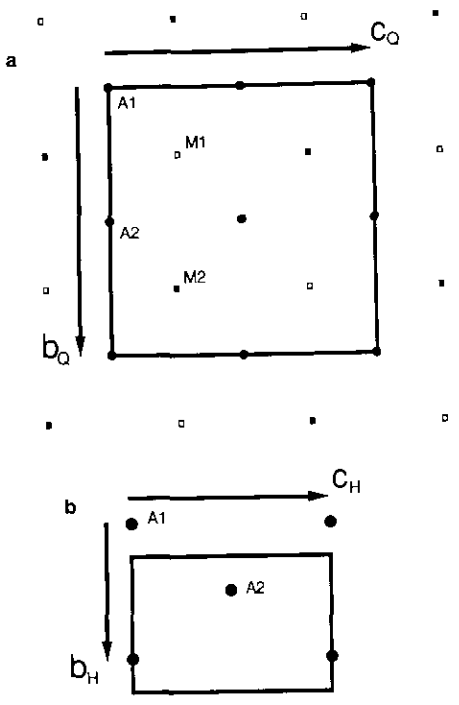

FIG. 1. Schematic representation of the parent substructures in a projection along the *a*-axis. In (a) the Q substructure with the 4^4 anion net and in (b) the H substructure or 3^6 anion net are shown. Note that $\mathbf{a}_Q = \mathbf{a}_H$, $\mathbf{b}_Q = 2\mathbf{b}_H$ and $\mathbf{c}_H = p/q\mathbf{c}_Q$ with $p < q$. Atoms *M*1 and *M*2 in (a) are above and below the plane ($\approx \pm\frac{1}{4}$), respectively, whereas all other atoms in (a) and (b) are in the plane.

Hyde and Andersson (8) defined two types of such Vernier structures—single and multiple Vernier structures whereby either one or more, respectively, additional anions are accommodated. Early work (10) suggested that the apparently long period superstructure phases were not truly long-range ordered but a result of the ordered intergrowth of several simpler "*basic unit orthorhombic phases*." Again, more recently (11), it has been suggested that the 27-times superstructure of Jung and Juza (3) is not genuinely long-range ordered but arises as a result of the coherent intergrowth of the $n = 5$ and $n = 6$ members of a presumed homologous series M_xA_{2x+1}. Typical medium resolution images taken with the **c*** axis excited, however, show no evidence for such an ordered intergrowth model although there is some evidence for occasional shifts and irregularities in the superlattice fringes (see Fig. 2). "*Notwithstanding earlier assumptions*", it has to be understood that "*multiple Vernier structures are not intergrowths of unit verniers*" (9). Examples of such Vernier phases include the yttrium oxide fluoride YO_xF_{3-2x}, $0.78 \leq x \leq 0.87$, system (12) and the zirconium nitride fluoride ZrN_xF_{4-3x}, $0.906 \leq x \leq 0.936$, system (3).

Related phases can be found in the zirconium niobium oxide system $Nb_2Zr_{x-2}O_{2x+1}$, $7.1 \leq x \leq 10.3$ (13–15) and in a number of lanthanide halide systems (16, 17). In these latter two systems, a somewhat different mechanism to the above was proposed to relieve the strain due to additional anions. This was the regular introduction of so-called antiphase boundaries (8) into the Vernier structures, described above, leading to the regular alternation within any one anion layer of 4^4 and 3^6 nets. It had been believed that Vernier-type systems with only one anion would always form these antiphase boundary type structures (i.e., with 3^6 and 4^4 nets alternating within each anion layer) to relieve the strain whereas compounds with two different anions would always form the originally described Vernier type structures upon anion ordering. Although this is true for the systems given above, a counter-example has been reported in the $Zr(O,F)_x$ system, $2.105 \leq x \leq 2.205$, (18).

In the YO_xF_{3-2x}, $0.78 \leq x \leq 0.87$, system each and every composition has its own but closely related structure—no diphasic region has ever been detected. An attempt was made to investigate this system in greater detail via transmission electron microscopy (TEM). Preliminary investigations, however, revealed that the phase was not particularly stable under electron beam irradiation. As the ZrN_xF_{4-3x}, $0.906 \leq x \leq 0.936$, phase had been found to be isostructural we started investigating this system in more detail. In a recent paper (19) a composite modulated structure approach to the structural description of this ZrN_xF_{4-3x} system was set out—involving two separate, mutually incommensurable subcells (the Q and H subcells described above). In this paper we investigate the compositional range of this phase, the composition dependence of the subcell periodicities and their relationship to the anion to cation ratio, as well as the crystal chemistry underlying the existence of such phases.

2. EXPERIMENTAL

2.1. Synthesis

The attempts to synthesize zirconium nitride fluoride follow, in principle, the method described by Jung and Juza (3). According to Eq. [1] ammonia has to be passed over ZrF_4 at a temperature of 580°C.

$$ZrF_4 + 4 \times NH_3 \xrightarrow{580°C} ZrN_xF_{4-3x} + 3 \times NH_4F \quad [1]$$

The main difficulty in synthesizing ZrN_xF_{4-3x} is exclusion of oxygen. At the reaction temperature of 580°C zirconium fluoride reacts preferably with oxygen to form either ZrO_2 or $Zr(O,F)_x$. As very long reaction times (up to 150 hr) in an "open" system are needed even small traces of oxygen are a severe problem. A further complication is that silica tubes react at the high temperature of synthesis with the NH_4F produced during the above

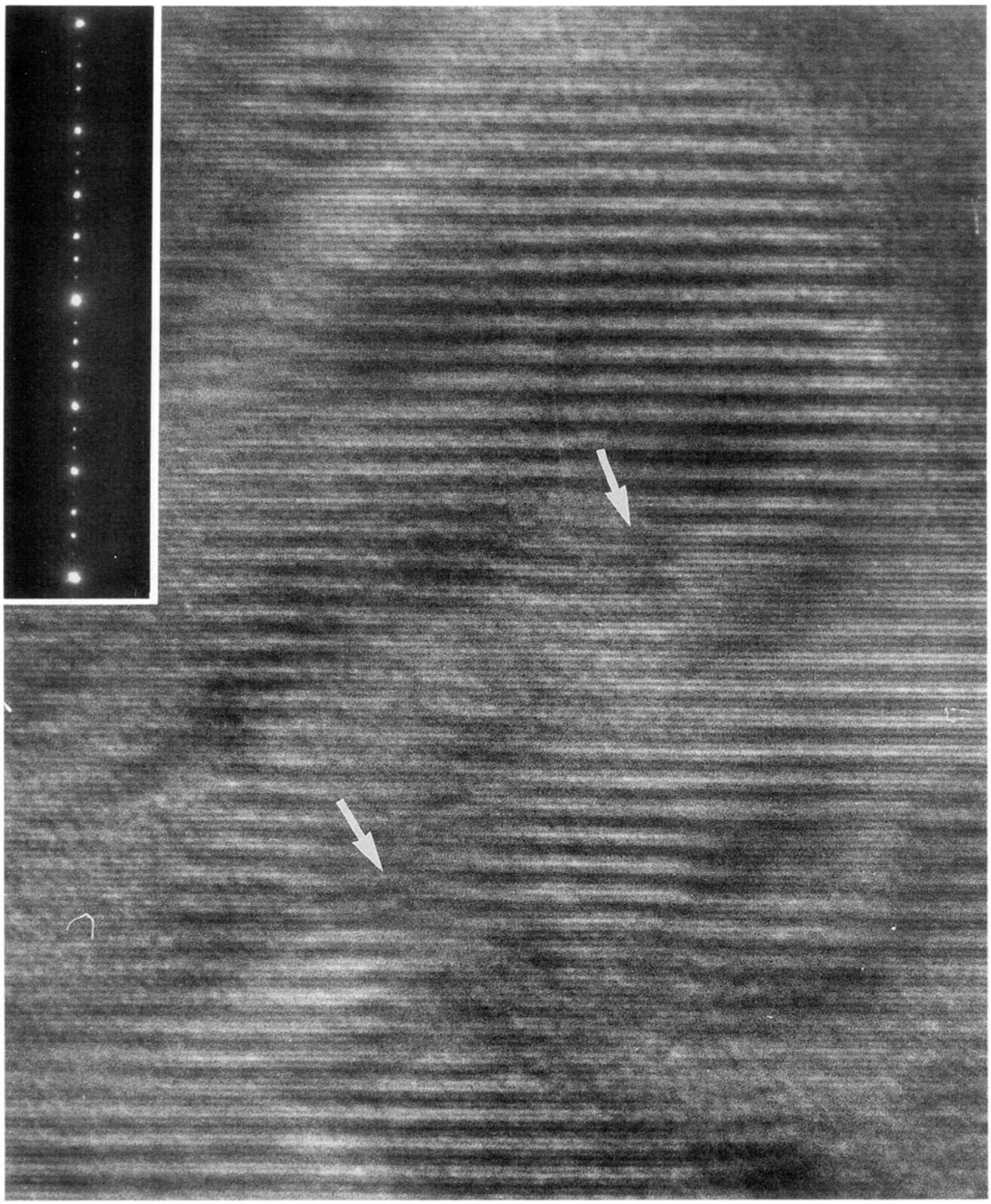

FIG. 2. Typical medium resolution image taken with the **c*** systematic row excited. The corresponding selected area diffraction pattern is inset. The fine (≈2.7 Å) fringes running vertically correspond to interference between the (0020) beam and the undiffracted beam while the larger scale (≈11.5 Å) fringes correspond to interference between the (0021) and (000-1) beams for this $\mathbf{q}_Q = -0.767\mathbf{c}_Q^*$ specimen (see Fig. 4(b) for indexing). There is no evidence for an ordered intergrowth model although there is some evidence for occasional shifts and irregularities in the superlattice fringes (arrowed).

reaction to form water. To prevent this the boat containing the fluoride has to be placed in a silver tube inside a silica tube. The silver tube must cover the hottest zone in the furnace.

The reactions were performed in the following way. ZrF_4 (Cerac, 99.9%) was finely ground under an Ar atmosphere then placed in an alumina boat in the silver-lined silica tube. ZrF_4 was heated for 3 days under a nitrogen atmosphere at 300°C to remove traces of water detected in the purchased material using X-ray powder diffraction (XRD). Subsequently anhydrous NH_3 (Matheson, 99.99%) was passed through the tube and the temperature slowly raised to 580°C. The total reaction times varied from 10 to 150 hr. The reactions were occasionally interrupted in order to analyse the product by XRD. In cases where the educt had not reacted sufficiently, the specimen was reground under Ar and then reheated to 580°C under NH_3.

The reaction times needed were a lot longer than the ones reported by Jung and Juza (3), presumably due to the higher reactivity of their ZrF_4 starting material. During the course of the reaction it was possible to assign XRD lines to zirconium oxy fluoride. These lines disappeared upon further treatment with NH_3 at 580°C and the final product showed only lines compatible with the patterns of zirconium nitride fluoride (3) or zirconium tetrafluoride.

This ammonolysis product was poorly crystallized and gave broad lines in Guinier films (see Fig. 3 a). TEM examination of various specimens showed the same poor crystallinity and inhomogeneity. Some of the specimens were therefore annealed in steel tubes to produce better crystallized powders and to grow large enough crystals for single crystal X-ray structure analysis. Annealing the initial product between 900 and 1100°C for 4 days to 3 weeks with varying amounts of ZrF_4 did indeed give much better crystallized specimens (see Fig. 3 b). It also enabled the previously reported composition range of the product phase to be investigated in more detail.

2.2. *Oxygen Content*

The appearance of zirconium oxy fluoride during the above reaction process, despite the effort to exclude oxygen, raised doubts as to the purity of the nitride fluoride. Unfortunately techniques capable of reliable quantitative analysis of light elements are not available. Recently Schlichenmaier *et al.* (11) detected some oxygen in their ammonolysis product via electron energy loss spectroscopy (EELS) and claimed a stoichiometry of $Zr_4N_3OF_5$. In an attempt to verify the presence or otherwise of such significant amounts of oxygen (~10% of the anion concentration), electron microprobe analysis of a homogeneous, well-annealed specimen was attempted.

Baddelyite (ZrO_2) and ZrF_4 were initially used as standards. It was not possible to analyze for nitrogen because of heavy absorption of the emitted nitrogen X-rays by the detector window. When specimens of $Zr_3O_2F_8$ and

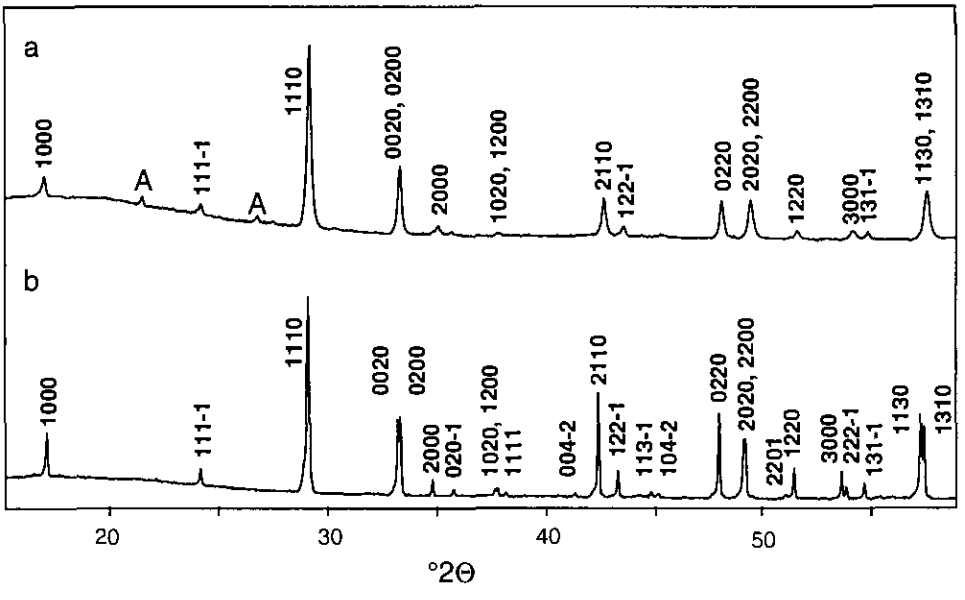

FIG. 3. Densitometer traces from Guinier films of (a) the ammonolysis product and (b) a specimen annealed at 1100°C for 1 week. The reflections of the ammonolysis product are much broader than the reflections of the annealed product (the reflections labelled A in (a) belong to $Zr_7O_9F_{10}$), and the weaker satellite reflections are only visible in the annealed product. It is not easy to observe the change in modulation wavevector as a function of composition by inspection of the data as there are no observable satellites higher than 2nd order and the Q substructure parent cell dimensions also change dramatically over the same composition range (see Section 3.5).

$Zr_7O_9F_{10}$ (20) were analyzed, however, it was found that the O/Zr ratio was calculating correctly, but that the F/Zr ratio was calculating ~20% and ~36% too high, respectively. A possible reason for this miscalculation of the F/Zr ratio could be that the *K* absorption edge for oxygen falls between the oxygen and fluorine $K\alpha$ lines so that oxygen atoms will strongly absorb the emitted fluorine X-rays making the usual corrections more difficult.

Subsequent analysis of our annealed $Zr(N,O,F)_x$ product phase gave an O/Zr ratio of ~4/13, i.e., it clearly contained a significant amount of oxygen and hence the phase really is a nitride oxide fluoride rather than a pure nitride fluoride. How quantitative is this ratio is another question, particularly as the *K* absorption edge for nitrogen falls between the nitrogen and oxygen $K\alpha$ lines so that nitrogen atoms would strongly absorb the emitted oxygen X-rays and, hence, provide a mechanism for miscalculation of the O/Zr ratio. Unfortunately there is no appropriate nitride oxide fluoride standard which can be used to allow a reliable composition of the phase to be determined.

Nonetheless, in agreement with the work of Schlichenmaier *et al.* (11), it is clear that the phase does contain a significant amount of oxygen. Jung and Juza (3) also found a small amount of oxygen in their specimen but chose to ignore it in the interpretation of their results. Instead of describing the phase as zirconium nitride fluoride it is appropriate to call it zirconium nitride oxide fluoride—$Zr(N,O,F)_x$.

2.3. XRD and Electron Diffraction

Specimens were examined by XRD using a Guinier–Hägg camera with monochromated $CuK\alpha_1$ radiation. An internal standard of Si (NBS No. 640) was used to calibrate the measurement of XRD films for least-squares refinement of the pseudotetragonal Q substructure unit cells dimensions ($a_Q \approx 5.12$–5.19 Å, $b_Q \approx 5.37$ Å, $c_Q \approx 5.38$ Å) as well as of the magnitude of the Q substructure primary modulation wave-vector, $\mathbf{q}_Q = -\mathbf{c}_Q^* + [\mathbf{c}_H^* - \mathbf{c}_Q^*]$, where $\mathbf{c}_H^*$ and $\mathbf{c}_Q^*$ are the reciprocal lattice dimensions of the parent H and Q substructures (see (19) and below). The material was further studied on JEOL 100CX and Philips EM430 transmission electron microscopes.

3. RESULTS AND DISCUSSION

3.1. Electron Diffraction Patterns

It will be shown below that the total anion to cation ratio of this phase is uniquely related to the ratio c_H^*/c_Q^* (or equivalently the Q substructure primary modulation wave-vector $\mathbf{q}_Q = -\mathbf{c}_Q^* + [\mathbf{c}_H^* - \mathbf{c}_Q^*]$) which can be measured directly from the appropriate diffraction pattern. Hence the composition range of this phase can not be discussed without a prior understanding of reciprocal space.

A [100] zone axis microdiffraction pattern and the corresponding selected area diffraction pattern (SADP) of a typical well-annealed specimen are shown in Fig. 4. The parent Q and H substructure reflections are indexed in (a) while a 4 integer notation, $(h, k, l, m)_Q^* = h\mathbf{a}_Q^* + k\mathbf{b}_Q^* + l\mathbf{c}_Q^* + m\mathbf{q}_Q^*$, based upon the more strongly scattering Q substructure, is used for indexing in (b). Note that when satellites of the *m*th order are referred to in what follows, it can be taken as referring to reflections of the form $(h, k, l, m)_Q^*$. Close inspection of (a) and (b) shows that the two components of the composite modulated structure (namely the parent Q and H substructures) are mutually incommensurable along their **c*** directions. By careful measurement of such diffraction patterns the ratio c_H^*/c_Q^* (or equivalently the Q substructure primary modulation wave-vector $\mathbf{q}_Q = -\mathbf{c}_Q^* + [\mathbf{c}_H^* - \mathbf{c}_Q^*]$) can be obtained.

Typical [010] and [001] zone axis patterns are not reported here as they have already been reported in a recent TEM study of this nominally ZrN_xF_{4-3x} system (19). In that study the appropriate superspace group symmetries characterizing the two components of the composite modulated structure—namely the Q and H substructures—were shown to be either $P:Abm2:1ss$ or $P:Abmm:1s - 1$ ($a_Q \approx 5.2$ Å, $b_Q \approx 5.4$ Å, $c_Q \approx 5.4$ Å, $\mathbf{q}_Q = -\mathbf{c}_Q^* + [\mathbf{c}_H^* - \mathbf{c}_Q^*]$) for the Q substructure and $B:Pmc2_1:s1s$ or $B:Pmcm:s1 - 1$ ($a_H = a_Q \approx 5.2$ Å, $b_H = \frac{1}{2}b_Q \approx 2.7$ Å, $c_H = p/q\ c_Q$ $(p < q) \sim 0.845c_Q \approx 4.56$ Å, $\mathbf{q}_H = \frac{1}{2}\mathbf{b}_H^* + [\mathbf{c}_H^* - \mathbf{c}_Q^*]$) for the H substructure respectively.

TEM investigation of the initial ammonolysis product showed almost exclusively a commensurate 4-times superstructure (i.e., $\mathbf{q}_Q = -\frac{3}{4}\mathbf{c}_Q^*$ or $c_H^*/c_Q^* = \frac{3}{4}$). This is consistent with the observations of Schlichenmaier *et al.* (11). The product, however, had only poor crystallinity and appeared to be rather inhomogeneous. The annealed specimens were different in that they were much better crystallized and the modulation wave-vector was clearly variable from preparation to preparation.

3.2. Magnitude of the Q Substructure Primary Modulation Vector and the Total Anion to Cation Ratio

The magnitude of the Q substructure primary modulation wave-vector, q_Q, for each composition has been determined from both XRD and electron diffraction patterns. From Guinier films $\mathbf{q}_Q/\mathbf{c}_Q^*$ was accurately derived using the $(1, 1, 1, -1)_Q^*$ and $(0, 2, 0, -1)_Q^*$ satellite reflections (see Section 3.1 above for the indexing notation). The value of $\mathbf{q}_Q/\mathbf{c}_Q^*$ derived from the XRD data, while in complete agreement with the value obtained from electron

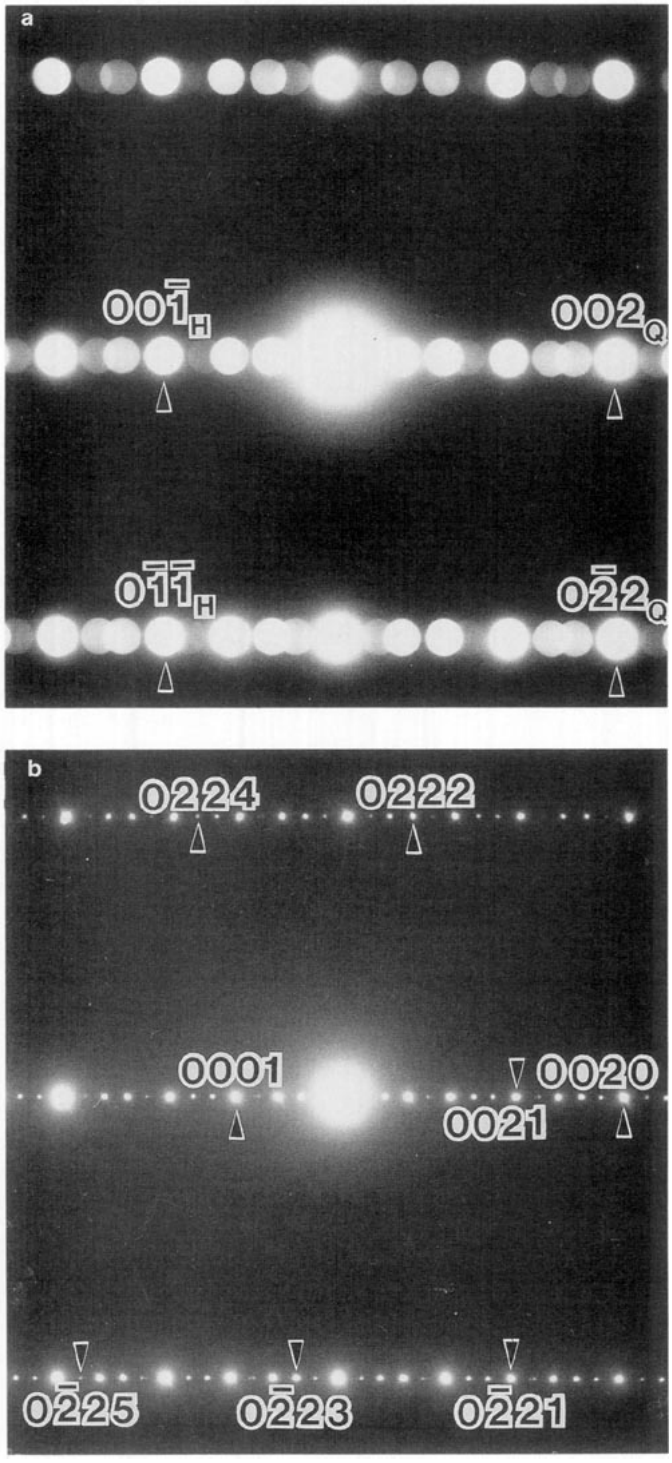

FIG. 4. A [100] zone axis microdiffraction pattern (a) and the corresponding selected area diffraction pattern (SADP) (b) of a typical well-annealed specimen. The parent Q and H substructure reflections are indexed in (a) while a four-integer notation, $(h, k, l, m)^*_Q = h\mathbf{a}^*_Q + k\mathbf{b}^*_Q + l\mathbf{c}^*_Q + m\mathbf{q}^*_Q$, based upon the more strongly scattering Q substructure, is used for indexing in (b). Close inspection of (a) and (b) shows that the parent Q and H substructures (the two components of the composite modulated structure) are mutually incommensurable along their $\mathbf{c}^*$ directions. By careful measurement of such diffraction patterns the ratio c^*_H/c^*_Q (or equivalently the Q substructure primary modulation wave-vector $\mathbf{q}_Q = -\mathbf{c}^*_Q + [\mathbf{c}^*_H - \mathbf{c}^*_Q]$) can be obtained.

diffraction patterns, could be determined with higher precision. A plot of the magnitude of $\mathbf{q}_Q/\mathbf{c}^*_Q$ versus the total anion to cation ratio for $Zr(N,O,F)_x$ is given in Fig. 5. The ratio of anions to cations for the three points marked by a square in Fig. 5 were obtained from structure refinements. The magnitude of $\mathbf{q}_Q/\mathbf{c}^*_Q$ is found to be linearly dependent on the total anion to cation ratio.

The reason for this linear relationship is the dependence of the relative periodicities of the Q and H substructures (see Fig. 1) upon stoichiometry. Consider, for example, a $\mathbf{c}$-axis length ratio of $\mathbf{c}_H/\mathbf{c}_Q = p/q$. Careful consideration of Fig. 1 shows that the corresponding stoichiometry must be given by $(MA)_pA_q$ or $MA_{1+q/p}$; i.e., the ratio of total anions to cations is given by $1 + q/p$. A $\mathbf{c}$-axis length ratio of $\mathbf{c}_H/\mathbf{c}_Q = p/q$, however, implies a ratio of $\mathbf{c}^*_H/\mathbf{c}^*_Q$ of q/p or a ratio of $\mathbf{q}_Q/\mathbf{c}^*_Q = (\mathbf{c}^*_H/\mathbf{c}^*_Q - 2)$ or $(q/p - 2)$; i.e., the ratio of total anions to cations for such systems is given by $(1 + \mathbf{c}^*_H/\mathbf{c}^*_Q)$ or $(3 + \mathbf{q}_Q/\mathbf{c}^*_Q)$.

Thus for $Y_7O_6F_9$ the wave-vector should be $-(6/7)\mathbf{c}^*_Q$ while, for $Zr_{108}N_{98}F_{138}$, the wave-vector should be $-(22/27)\mathbf{c}^*_Q$. This is true in both cases. With a wave-vector of $-(7/9)\mathbf{c}^*_Q$ the composition should, therefore, be $Zr_9(N,O,F)_{20}$, i.e., $ZrA_{2.22}$. This has been confirmed with the results of a preliminary structure analysis of a commensurate 9-times superstructure. The composition $Zr_4ON_3F_5$, as given by Schlichenmaier *et al.* (11), follows the same rule, because the wave-vector is $-(3/4)\mathbf{c}^*_Q$ as expected for a composition with an excess of one H subcell per four Q subcells. As the formula holds for these various types of compounds it seems that the magnitude of the primary modulation wave-vector $\mathbf{q}_Q/\mathbf{c}^*_Q$ is determined by the anion to cation ratio, and is independent of what sort of anions and cations are involved.

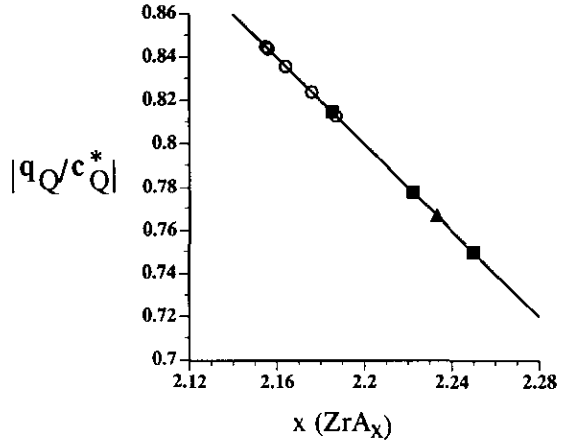

FIG. 5. The magnitude of the wave-vector $|\mathbf{q}_Q/\mathbf{c}^*_Q|$ is given as a function of the total anion to cation ratio. The squares represent values taken from structure refinements (3, 11) and the regression line is calculated from these values. The open circles represent values extracted from Table 3 in (3).

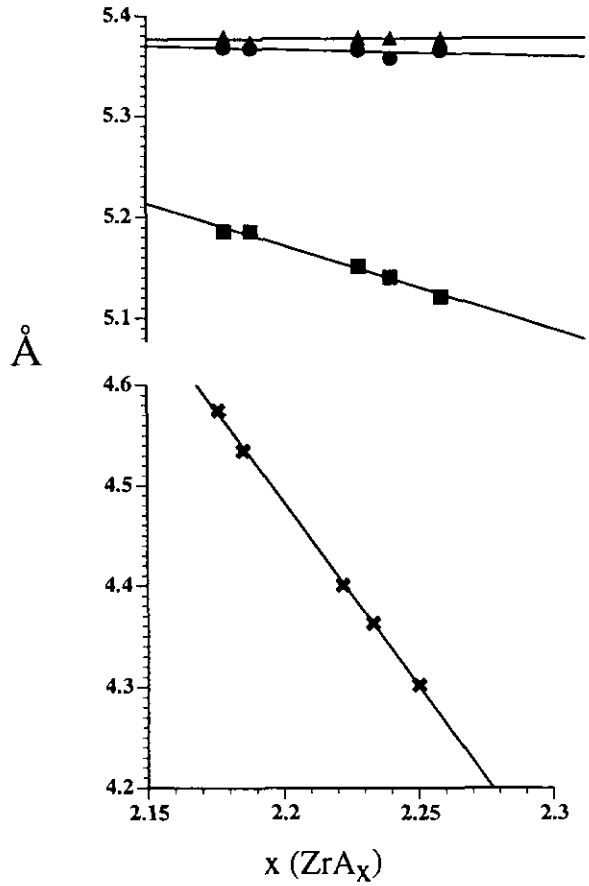

FIG. 6. Plot of the $\mathbf{a}_Q$ (squares), $\mathbf{b}_Q$ (circles), $\mathbf{c}_Q$ (triangles), and $\mathbf{c}_H$ (crosses) substructure unit cell dimensions as a function of the total anion to cation ratio. There is a steady decrease in the $\mathbf{a}_Q$ subcell dimension as the anion to cation increases whereas the subcell $\mathbf{b}_Q$ dimension varies much less and the subcell $\mathbf{c}_Q$ dimension is more or less constant to within the standard deviations. The $\mathbf{c}_H$ substructure unit cell dimension decreases dramatically as a function of increasing anion to cation ratio showing an ~8% change across the solid solution field.

3.3. *Phase Relationships*

The phase relationships, although similar, were in some respects substantially different from the results Jung and Juza reported (3). The product we synthesized through ammonolysis of ZrF_4 is much more anion-rich than the specimens they reported. Assuming the validity of the relation between composition and magnitude of modulation wave-vector (see the discussion given in Section 3.2 above and Fig. 5) the composition of the initial ammonolysis product would be $Zr(N,O,F)_{2.25}$—clearly well outside the phase region $0.906 \leq x \leq 0.936$ (equivalent to $Zr(N,O,F)_{2.128}$ to $Zr(N,O,F)_{2.188}$) reported by Jung and Juza. This assignment has been supported by the recent paper of Schlichenmaier *et al.* (11). Their initial ammonolysis product is apparently the same as reported here with composition $Zr_4ON_3F_5$, i.e., $ZrA_{2.25}$.

Whereas Jung and Juza reported a change in composition of their ammonolysis product with reaction time (3), we found that the wave-vector, and therefore the composition of this initial product, did not vary. There was only a difference in yield. However, apart from briefly mentioning the change in composition, Jung and Juza did not further comment on their ammonolysis product.

Jung and Juza (3) noticed much variability in the precession photographs of single crystals of their material. They defined "reduced distances" between reflections, which means that they normalized the distances between neighboring reflections with respect to the parent subcell dimensions. We interpret the results of Table 3 in Ref. 3 in a different way. The sum of the two principal reduced distances they report for each composition is equal to the magnitude of our modulation vector $\mathbf{q}_Q/\mathbf{c}_Q^*$ (e.g., 0.373 + 0.440 = 22/27 for $Zr_{108}N_{98}F_{138}$). By this means, from their Table 3, it is clear that they managed to synthesize specimens with anion to cation ratios ranging from 2.155 to 2.187. Given the virtually continuous variability in the magnitude of the primary modulation vector $\mathbf{q}_Q/\mathbf{c}_Q^*$ observed in this present study as a function of synthesis conditions, it is clear that this $Zr(N,O,F)_x$ system is best treated as a single phase solid-solution. It would appear that there is a complete solid solution for $Zr(N,O,F)_x$ from $x = 2.128$ to 2.250. It may indeed even be possible to further expand this composition range via appropriate synthesis conditions.

Unfortunately it is not easy to control the formation of a particular composition in this $Zr(N,O,F)_x$ phase field. As the ammonolysis reaction is carried out in an open system the formation of the product is controlled by the mutual relationship of the partial pressures of ZrF_4, NH_3, and oxygen at the reaction temperature. To obtain products with more easily controllable composition solid state reaction between zirconium nitride and zirconium fluoride is certainly the best way to choose. Jung and Juza (3) reported problems with this route but we are reexamining this synthetic possibility.

3.4. *Unit Cell Dimensions*

Unit cell dimensions of the A-centered orthorhombic parent Q substructure throughout the solid-solution field were determined from XRD patterns. A least-squares refinement of parent unit cell data out to 63° 2θ for $CuK\alpha_1$ was used. Fig. 6 shows a plot of the $\mathbf{a}_Q$, $\mathbf{b}_Q$, and $\mathbf{c}_Q$ substructure unit cell dimensions as well as the $\mathbf{c}_H$ substructure unit cell dimension as a function of the total anion to cation ratio. The values for two compositions of Jung and Juza (3) are incorporated in this plot. There is a steady decrease in the $\mathbf{a}_Q$ subcell dimension as the anion to cation ratio increases whereas the subcell $\mathbf{b}_Q$ dimension varies much less and the subcell $\mathbf{c}_Q$ dimension is more or less constant to within the standard deviations. On the other hand, the $\mathbf{c}_H$ substructure unit cell dimension decreases

dramatically as a function of increasing anion to cation ratio showing an ~8% change across the solid solution field. Clearly all the variability in the c_H/c_Q ratio as a function of composition is taken up by the H, rather than the Q, substructure.

3.5. *Apparent Valence Calculations*

In their respective reported structure refinements, neither Bevan *et al.* (12) nor Jung and Juza (3) distinguished between their anions (O, F) and (N, F), respectively. As N, O, F are neighboring elements it is rather difficult to distinguish between them by X-ray structure analysis only. One of the most useful ways of checking the chemical plausibility of a structure refinement is via the calculation of apparent valences (AVs) using the bond length–bond valence approach (21–23). The relationship between the length of a bond (r^{ij}) and its valence (s^{ij}) is given as $s^{ij} = \exp[(r_0^{ij} - r^{ij})/B]$. Brown and Altermatt (22) have refined the parameters r_0^{ij} and B for over 750 atom pairs and listed the 141 most accurately determined values for r_0^{ij}. They find empirically that B can be set to a constant, namely 0.37 Å. The apparent valence (AV) of atom i, V_i', is then obtained as a sum over all the neighboring bond valences, i.e., $V_i' = \Sigma_j s^{ij}$. If these AVs agree (i.e., within ± 0.2 valence units) with the theoretically expected valences (4 for Zr, 3 for N, 2 for O, and 1 for F) one can have confidence that the structure has been reliably determined. By the calculation of AVs (24) for the structure of $Zr_7O_9F_{10}$ (25), for example, it has proved possible not only to confirm the chemical plausibility of the published structure but also to identify those anion sites which are occupied by O, those occupied by F, and those sites occupied by a mixture of O and F (20).

Papiernik and Frit (18) deduced from AVs for $Y_7O_6F_9$ and $Zr_{108}N_{98}F_{138}$ that the smaller fluorine ions are located in the 3^6 nets while the larger oxygen and nitrogen ions, respectively, are located in the 4^4 nets of the structures. However, they only used bond valence parameters for Y–O and Zr–F. As there are as many anions in the 4^4 net as metals some fluorine ions have to be distributed on the 4^4 nets of both structures, in order to satisfy the stoichiometry. The question remains as to whether these 4^4 net fluorine ions are fully ordered, partially ordered or randomly distributed. Papiernik and Frit did not further comment on their calculated numbers. Bevan *et al.* gave the AVs they had calculated for $Y_6O_5F_8$ (12) and suggested that the 4^4 net fluorine ions may be located on a specific site in the supercell in such a way as to obtain the correct stoichiometry. These results were somewhat misleading as the r_0^{ij} value for the bond between Y and F used deviated significantly from the currently accepted value.

A systematic examination of AVs for the reported crystal structure of $Zr_{108}N_{98}F_{138}$ (3), the four structures reported for the yttrium oxide fluoride system (12) and the recently published structure of $Zr_4ON_3F_5$ (11) is very informative from a crystal chemical point of view. For $Y_5O_4F_7$, $Y_6O_5F_8$, and $Y_7O_6F_9$ the results are very convincing. In the 3^6 net there are definitely only fluorine ions. It also seems clear from these AVs that the fluorine ions which have to be placed in the 4^4 net are randomly distributed, rather than partially ordered, over all anion positions in this net. In order to save space only the AVs calculated from the reported crystal structure of $Y_7O_6F_9$ (12) are given in Table 1 as an example. The conclusion that can be drawn from the AVs for the YO_xF_{3-2x} system, however, are always the same. In the case of $Y_{17}O_{14}F_{23}$ the AVs are not in as good agreement, due presumably to the slightly worse structure determination, but there is still no evidence for anion ordering in the 4^4 net.

Jung and Juza used the atomic form factors of O^{2-} for all anion positions in their structure refinement of $Zr_{108}N_{98}F_{138}$ (3). The AVs calculated from this reported crystal structure again strongly suggest that only F occupies sites in the 3^6 net. The sites in the 4^4 net seem to be occupied by nitrogen with a small amount of fluorine randomly distributed in order to obtain the correct composition. Although the AVs are about 15% too high for the Zr and N/F positions they have the expected values for the F positions. The numbers range from 4.38 to 4.60 for Zr, from 3.31 to 3.56 for N/F and from 0.86 to 1.00 for F. Substituting some O into the N/F positions, not surprisingly, reduces the AVs of the neighboring Zr's. The AV of the O, however, still remains too high. Whether this deviation from the expected valences is genuine, indicates

TABLE 1
Apparent Valences for $Y_7O_6F_9$

Sites	Model 1[a]	Model 2[b]	All O[c]	All F[d]
Y1	3.003	2.919	3.353	2.491
Y2	3.066	2.977	3.403	2.528
Y3	2.912	2.836	3.295	2.447
Y4	3.392	3.294	3.766	2.797
*X*1	2.035	1.949	2.035	1.512
*X*2	1.975	1.891	1.975	1.467
*X*3	2.053	1.966	2.053	1.525
*X*4	2.001	1.917	2.001	1.487
*X*5	0.899	0.899	1.211	0.899
*X*6	0.923	0.923	1.242	0.923
*X*7	0.922	0.922	1.241	0.922
*X*8	0.918	0.918	1.236	0.918
*X*9	0.837	0.837	1.127	0.837

[a] Coordinates from (12); O on *X*1–*X*4 (4^4 net), F on *X*5–*X*9 (3^6 net); R_0 Y–O = 2.014; R_0 Y–F = 1.904 (24).
[b] 4^4 positions occupied by 1/7 F and 6/7 O; R_0 Y–O/F = 1.998; expected valence: 1.857.
[c] All anions O.
[d] All anions F.

TABLE 2
Apparent Valences for $Zr_4ON_3F_5$

Sites	Model[a]	All N[b]	All O[c]	All F[d]
Zr1	4.191	5.970	3.671	2.933
Zr2	4.806	6.574	4.037	3.226
Zr3	3.926	5.150	3.227	2.578
Zr4	4.781	5.959	3.733	2.983
N1	3.927	3.927	2.460	1.966
N2	3.887	3.887	2.435	1.946
N3	3.403	3.403	2.132	1.704
F4	1.083	2.163	1.355	1.083
O5	1.905	3.041	1.905	1.522
F6	0.885	1.878	1.108	0.885
F7	1.051	2.100	1.315	1.051
F8	0.779	1.556	0.975	0.779
F9	0.784	1.698	0.982	0.784

[a] Coordinates from (11); N, O on 4^4, F on 3^6; R_0 Zr–N = 2.110; R_0 Zr–O = 1.937; R_0 Zr–F = 1.854 (24).
[b] All anions N.
[c] All anions O.
[d] All anions F.

a problem with the refinement or is due to an error in the r_0^{ij} parameter for $Zr^{4+} - N^{3-}$ (2.110 Å (24)) is far from clear. Again the distribution of the numbers does not indicate a preference for the fluorine ions to occupy a particular site in the 4^4 net. The probability, as discussed above, that oxygen ions also occur in the 4^4 net considerably complicates this interpretation.

In the case of the recent structure refinement of $Zr_4ON_3F_5$ from neutron powder diffraction data, complete anion ordering has been reported (11). Although some of the atom positions give reasonable AVs (see Table 2) the structure must be considered doubtful as Zr2, Zr4, N1, and N2 are dramatically overbonded. Adjustment of the listed r_0^{ij} parameter for $Zr^{4+} - N^{3-}$ (which may well be unreliable due to the extreme paucity of well-defined zirconium nitrides) will not rectify the discrepancies between calculated and expected valences. This probably reflects the problems—mentioned by Schlichenmaier *et al.* (11)—with the structure solution and refinement. The ammonolysis product is unlikely to be sufficiently homogeneous to obtain a good structure refinement from powder data. Therefore, it is not possible to deduce from this refinement whether anion ordering in the 4^4 net occurs.

4. CONCLUSIONS

While the exact composition of "zirconium nitride fluoride" is extremely difficult to determine, due to variable substitution, $2O^{2-} \Leftrightarrow N^{3-} + F^-$, the total anion to cation ratio can nonetheless be uniquely determined from careful measurement of diffraction patterns and can range from 2.12 right up to 2.25. Note that for the same anion to cation ratio, a range of $2O^{2-} \Leftrightarrow N^{3-} + F^-$ substitution may occur. Apparent valence considerations (see Section 3.5), however, strongly suggest that only Fs occupy the 3^6 net. If this is the case, then the level of substitution is limited, e.g., consider $Zr_9(N,O,F)_{20}$. A "pure" nitride fluoride with this anion to cation ratio would have stoichiometry $Zr_9N_8F_{12}$, i.e., $Zr_9(N_8F)F_{11}$. Complete occupancy of the 3^6 net by F implies that a maximum of one substitution of the above form can then occur leading to an extreme stoichiometry of $Zr_9(N_7O_2)F_{11}$. AV calculations further suggest that there is no anion ordering within the 4^4 net and, hence, any stoichiometry between the above limits is, at least in principle, possible.

The material we have synthesized shows the same features as that reported by Jung and Juza (3) and although more anion rich is clearly part of the same solid solution field. The apparently continuous variability in the anion to cation ratio, as measured from diffraction patterns, strongly supports the description of this phase as an incommensurate, compositely modulated structure, with a continuously variable, composition-dependent, primary modulation wave-vector. Understanding of features such as the composition dependence of the Q and H substructure cell dimensions requires structure solutions in such terms across the solid solution field. These structure solutions will clearly benefit from using the anion ordering scheme shown above.

ACKNOWLEDGMENTS

The authors want to thank Mr. Nick Ware and Mr. Peter Barlow for assistance with the electron microprobe work, Mr. Keith Owen for assistance with the densitometer traces, and Dr. John G. Thompson for helpful discussions.

REFERENCES

1. R. Juza, R. Sievers, and W. Jung, *Naturwissenschaften* **53,** 551 (1966).
2. S. Andersson, *Ark. Kemi* **26,** 521 (1967).
3. W. Jung and R. Juza, *Z. Anorg. Allg. Chem.* **399,** 129 (1973).
4. C. Wüstefeld, T. Vogt, U. Löchner, J. Strähle, and H. Fueß, *Angew. Chem.* **100,** 1013 (1988).
5. N. E. Brese and M. O'Keeffe, *Struct. Bonding* **79,** 307 (1992).
6. D. J. M. Bevan and A. W. Mann, *Acta Crystallogr. Sect. B* **31,** 1406 (1975).
7. B. G. Hyde, A. N. Bagshaw, S. Andersson, and M. O'Keeffe, *Ann. Rev. Mater. Sci.* **4,** 43 (1974).
8. B. G. Hyde and S. Andersson, "Inorganic Crystal Structures," pp. 311–318. Wiley, New York, 1989.
9. E. Makovicky and B. G. Hyde in "Non-Commensurate Layered Structures" (A. Meerschaut, Ed.), pp. 1–100. Trans Tech Publications, 1992.
10. A. W. Mann and D. J. M. Bevan, *J. Solid State Chem.* **5,** 410 (1972).
11. R. Schlichenmaier, E. Schweda, J. Strähle, and T. Vogt, *Z. Anorg. Allg. Chem.* **619,** 367 (1993).

12. D. J. M. Bevan, J. Mohyla, B. F. Hoskins, and R. J. Steen, *Eur. J. Solid State Inorg. Chem.* **27,** 451 (1990).
13. J. Galy and R. S. Roth, *J. Solid State Chem.* **7,** 277 (1973).
14. J. G. Thompson, R. L. Withers, P. J. Sellar, P. J. Barlow, and B. G. Hyde, *J. Solid State Chem.* **88,** 465 (1990).
15. R. L. Withers, J. G. Thompson, and B. G. Hyde, *Acta Crystallogr. Sect. B* **47,** 166 (1991).
16. C. Rinck, Ph.D. thesis, University of Karlsruhe, 1982.
17. R. Bachmann, Ph.D. thesis, University of Karlsruhe (1987).
18. R. Papiernick and B. Frit, *Acta Crystallogr. Sect. B* **42,** 342 (1986).
19. R. L. Withers, S. Schmid, and J. G. Thompson, *Acta Crystallogr. Sect. B* **49,** 941 (1993).
20. J. G. Thompson, R. L. Withers, and C. J. Kepert, *J. Solid State Chem.* **95,** 111 (1991).
21. I. D. Brown, *Chem. Soc. Rev.* **7,** 359 (1978).
22. I. D. Brown and D. Altermatt, *Acta Crystallogr. Sect. B* **41,** 244 (1985).
23. M. O'Keeffe, *Struct. Bonding* **71,** 161 (1989).
24. EUTAX7, N. E. Brese and M. O'Keeffe, *Acta Crystallogr. Sect. B* **47,** 192 (1991).
25. B. Holmberg, *Acta Crystallogr. Sect B* **26,** 830 (1970).